IRANIAN JOURNAL OF CATALYSIS

Synthesis of 14*H*-dibenzo[*a.j*]xanthenes using Co@pyr/APTZCMNPs as a novel heterogeneous nanocatalyst

Esmayeel Abbaspour-Gilandeh*, Mehraneh Aghaei-Hashjin

Young Researchers and Elites Club, Ardabil Branch, Islamic Azad University, Ardabil, Iran.

ABSTRACT

Co@pyr/APTZCMNPs was synthesized, and some of its characteristic analyses, such as Fourier transform infrared spectroscopy (FTIR), thermogravimetric analysis (TGA), scanning electron microscopy (SEM), energy dispersive X-ray (EDX) and X-ray diffraction (XRD) were investigated. The results indicated that this heterogeneous catalyst was an excellent and reusable system to synthesize of 14*H*-dibenzo[*a.j*]xanthene derivatives through a one-pot condensation of *β*-naphthol and arylaldehydes at 90 °C under solvent-free conditions. Due to the magnetic nature of the catalyst, it could be easily recovered by an external magnetic field and comfortable reused at least five times without loss of its catalytic activity. High yields of the desired product, easy recovery of the catalyst and solvent-free conditions were some of the advantages of our methodology.

Keywords: Heterogeneous Catalyst, β-naphthol, 14H-dibenzo[a.j]xanthenes, Solvent-free conditions.

1. Introduction

Recently, magnetic nanoparticles (MNPs) and study of their utilization in the production of fine chemical synthesis have gained a major area of research owing to their high performance, large surface area, easy retrievability and reusability by implying an external magnet [1-5]. The usage of nanomagnetic catalysts in organic synthesis is an interesting procedure to access green catalysis, which is suitable for the environment and highly interesting in different processes of chemical transformations due to the very small size of nanoparticle materials and easy dispersion in solution [6-7]. Most significantly, this class of nanoparticles has been widely used in adsorption, electrodes, gas sensors, MRI contrast agents and hyperthermia treatment for cancer [8-12].

The synthesis of xanthene derivatives, especially benzoxanthenes with their biological and therapeutic properties such as antibacterial [13] antiviral [14] and anti-inflammatory activities [15] as well as in photodynamic therapy [16] has emerged as a powerful tool in organic synthesis.

These activities heterocyclic compounds due to their useful spectroscopic properties have been applied as dyes [17] in fluorescent materials to visualize biomolecules [18] and in laser technologies [19]. The formation of 14*H*-dibenzo[*a.j*]xanthenes and related products is based on the one-pot condensation of β-naphthol with 2-naphthol-1-methanol [20], formamide [21], sulfonic acid [22] and carbon monoxide [23]. Recently, several elegant multicomponent strategies to synthesize of 14*H*-dibenzo[*a.j*]xanthenes by multi-component reactions utilizing catalysts have been reported [24-28]. Although some of these methods afford good-to-high yields of the corresponding 14*H*-dibenzo[*a.j*] xanthenes, many of them have certain drawbacks, including low yields, prolonged reaction time, use of an excessive of reagents/catalysts and use of toxic organic solvents.

2. Experimental

2.1. General

All chemical materials were purchased from Aldrich and Merck Chemical Company and used without further purification. The melting points were performed with an Electrothermal 9100 apparatus and were uncorrected. Infrared spectra was recorded on a

*Corresponding author email: abbaspour1365@yahoo.com
Tel.: +98 45 3333 2238; Fax: +98 45 3336 3199

PerkinElmer PXI instrument. The purity determination of the product and reaction monitoring was accomplished using a TLC on silica gel PolyGram SILG/UV 254 plates. The IR spectra were obtained using a PerkinElmer PXI instrument in KBr wafers. Thermogravimetric analysis (TGA) was recorded on a Linseis SATPT 1000 thermoanalyzer instrument. X-ray diffraction (XRD) measurements were done the 2θ range of 10-80° at room temperature on a Siemens D-500 X-ray diffractometer (Munich, Germany), using Ni-filtered Cu-Kα radiation (λ= 0.15418 nm). Scanning election microscopy (SEM) was performed on a SEM-LEO 1430VP. Elemental analyses were accomplished using a Carlo-Erba EA1110CNNO-S analyzer and agreed (within 0.30) with the calculated values. Inductively coupled plasma atomic emission spectrometry (ICP-AES) measurements were obtained using a VARIAN VISTA-MPX. Transmission electron microscopy was performed by the Philips CM30 TEM.

2.1.1. General procedure for the preparation of xanthene derivatives

A mixture of β-naphthol (2 mmol), benzaldehyde (1 mmol) and Co@pyr/APTZCMNPs (10 mg) was heated at 90 °C under solvent-free conditions. The reaction progress was monitored by thin-layer chromatography (TLC). After completion of the reaction, the mixture was washed with water (2×15 mL) and then recrystallized from EtOAc/n-hexane (1:3) to afford the pure product (89%). The same procedure was also utilized for the other products listed in Table 2.

2.1.2. Preparation of Fe₃O₄ nanoparticles (MNPs)

FeCl$_3$.6H$_2$O (2.36 g) and FeCl$_2$.4H$_2$O (0.86 g) were dissolved in 40 mL distilled water under stirring at 90 °C and continuous flow of argon gas. This solution was maintained at 90 °C for 30 min, and then 10 mL of ammonia (25%) was added drop-wise to the reaction mixture until a dark suspension solution was obtained. Extraction of the solution by an external magnet afforded the black MNPs product. Prepared nanoparticles were washed with deionized water repeatedly and dried at 60 °C for 12 hours.

2.1.3. Preparation of Fe₃O₄@ZrO₂ nanoparticles (ZCMNPs)

One g of Zirconium (IV) oxychloride octahydrate (ZrOCl$_2$.8H$_2$O) (1 g) was dissolved in 50 mL of ethanol to form a clear solution and added drop-wise to 50 mL aqueous suspension of 5 g Fe$_3$O$_4$ MNPs

(stirred with the help of ultrasonication for 1 hours). Then, this mixture was stirred for 12 hours, and the ethanol was evaporated to become a dry powder, which was maintained overnight in an air oven at 90 °C.

2.1.4. Functionalization of Fe₃O₄@ZrO₂ with 3-aminopropyltriethoxysilane (APTZCMNPs)

Fe$_3$O$_4$@ZrO$_2$ nanoparticles (1 g) were suspended in dry toluene (20 ml) under nitrogen atmosphere. To this solution, 3-aminopropyltriethoxysilane (APT, 2 mL) was slowly added and the mixture was refluxed for 24 hours. After this period, the resulted precipitates were separated by a permanent magnet and washed several times with ethanol and distilled water to remove impurities. Finally, the produced solid nanoparticles were dried under vacuum oven.

2.1.5. Functionalization of APTZCMNPs with 2-pyridinecarboxaldehyde (pyr/APTZCMNPs)

In a typical reaction, 2.0 g of APTZCMNPs was suspended in 20 ml dry CH$_2$Cl$_2$ and the mixture was stirred for 30 minutes; then, 0.245 of 2-pyridinecarboxaldehyde was added to the reaction mixture and the mixture was refluxed for 8 hours. The precipitates (pyr/APTZCMNPs) were removed from the solvent by filtration, washed with water and then dried under vacuum oven.

2.1.6. Preparation of Co@pyr/ APTZCMNPs

To prepare of Co@pyr/APTZCMNPs catalyst, pyr/APTZCMNPs (2 g) was dispersed in CH$_2$Cl$_2$ (20 mL) for 30 minutes using ultrasound. CoCl$_2$ (0.25 mmol) was added to the mixture and the mixture was stirred at 80 °C for 24 hours. After 24 hours, Co@pyr/APTZCMNPs was separated by an external magnet and repeatedly washed with distilled water and then dried under vacuum oven. All stages of the Co@pyr/APTZCMNPs synthesis are exhibited in Scheme 1.

3. Results and Discussion

3.1. Synthesis and characterization of catalyst

3.1.1. FTIR analysis

FTIR spectra of the ZCMNPs, APTZCMNPs, pyr/APTZCMNPsand Co@pyr/APTZCMNPs are shown in Fig. 1. In the case of ZCMNPs, the observed peak at 3436 cm^{-1} is relevant to the hydroxyl units attached to iron.
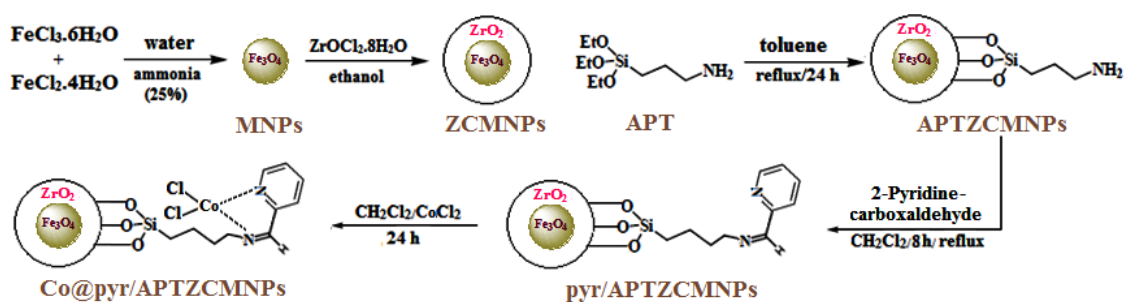
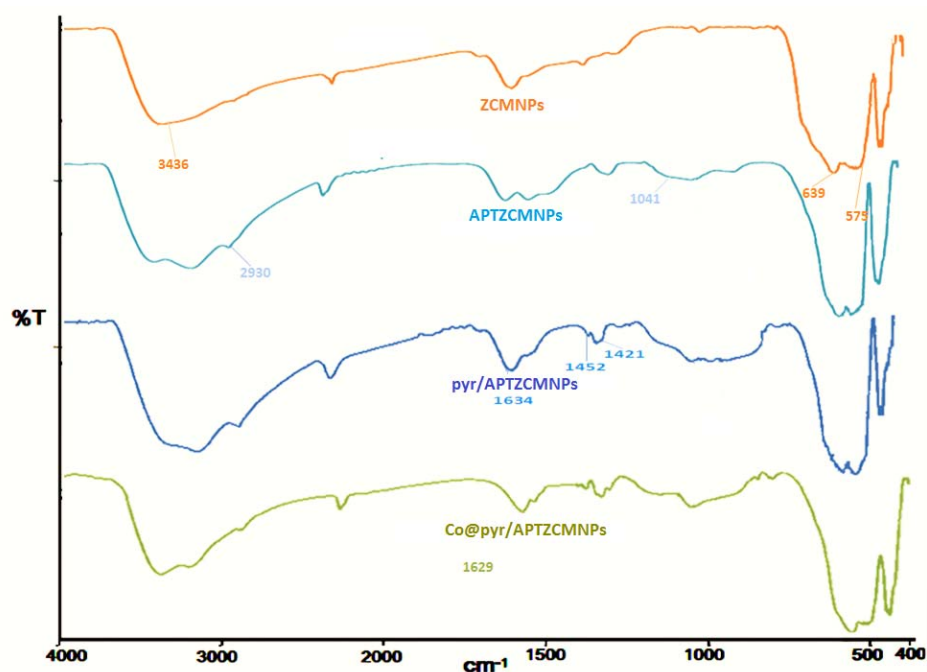**Scheme 1.** All stages of the Co@pyr/APTZCMNPs synthesis.

Fig. 1. FTIR spectra of ZCMNPs, APTZCMNPs, pyr/APTZCMNPs and Co@pyr/APTZCMNPs.

The peaks appearing in the 575 and 639 cm^{-1} can be attributed to the Fe-O and Zr-O stretching vibrations, respectively. In the spectrum of the APTZCMNPs, The band at 1041 cm^{-1} can be collectively assigned to Si-O stretching vibrations. Also, the aliphatic C-H stretching vibrations of propyl groups emerged at 2930 cm^{-1}. The FT-IR spectrum of pyr/APTZCMNPs, show the peaks at 1634 and 1400- and 1500 cm^{-1} for C=N and C=C bond, respectively. It should be noted that the C=N band is shifted from 1634 cm^{-1} in pyr/APTZCMNPs to 1629 cm^{-1} in Co@pyr/APTZCMNPs implying that C=N bond is coordinated to Co through the nitrogen's lone pair.

3.1.2. TGA analysis

In the TGA curve of Co@pyr/APTZCMNPs, the first weight loss stage (below 235 ºC) is concerned with the evaporation of adsorbed water and solvent molecules on the catalyst surface, while another considerable weight loss stage beginning at approximately 370 ºC was due to the decomposition of organic groups and ligands (Fig. 2).
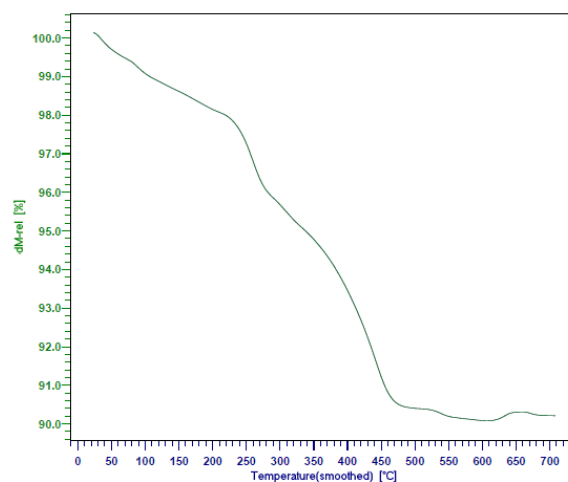

Fig. 2. TGA curve of Co@pyr/APTZCMNPs.

3.1.3. XRD analysis

The MNPs, pyr/APTZCMNPs and Co@pyr/APTZCMNPs magnetic nanoparticles were investigated by X-ray powder diffraction (XRD). The peaks were compatible with MNPs phase (JCPDS card No. 79-0417), indicating the protection of the cubic reverse spinel structure of magnetic iron oxide nanoparticles during coating and functionalization. There were, however, no characteristic peaks of Co species in the XRD pattern of Co@pyr/APTZCMNPs as compared with those of pyr/APTZCMNPs (Fig. 3).

3.1.4. SEM analysis

The surface morphology, size distribution and particle shape of the nanoparticles were determined by scanning electron microscopy (SEM). The SEM micrographs showed that the Co@pyr/APTZCMNPs were spherical with the mean diameter of approximately 52 nm (Fig. 4).
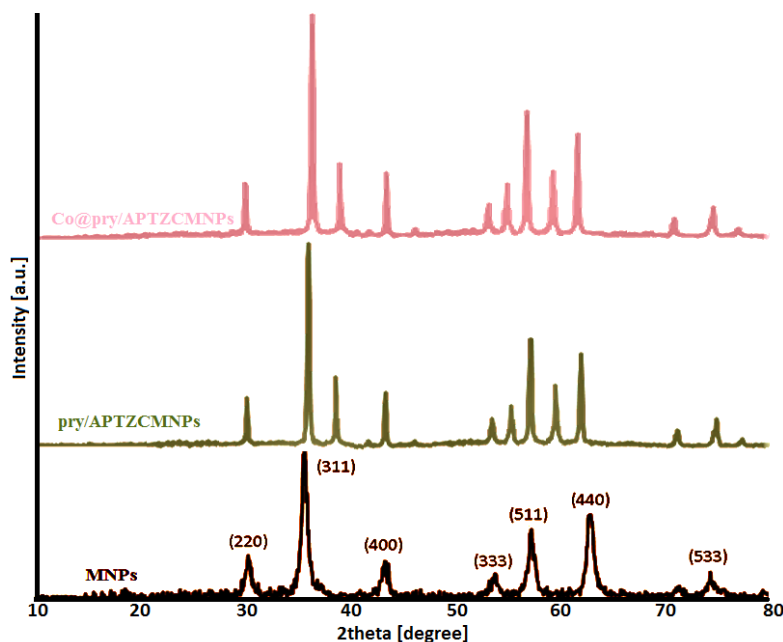

Fig. 3. XRD patterns of MNPs, pyr/APTZCMNPs and Co@pyr/APTZCMNPs.
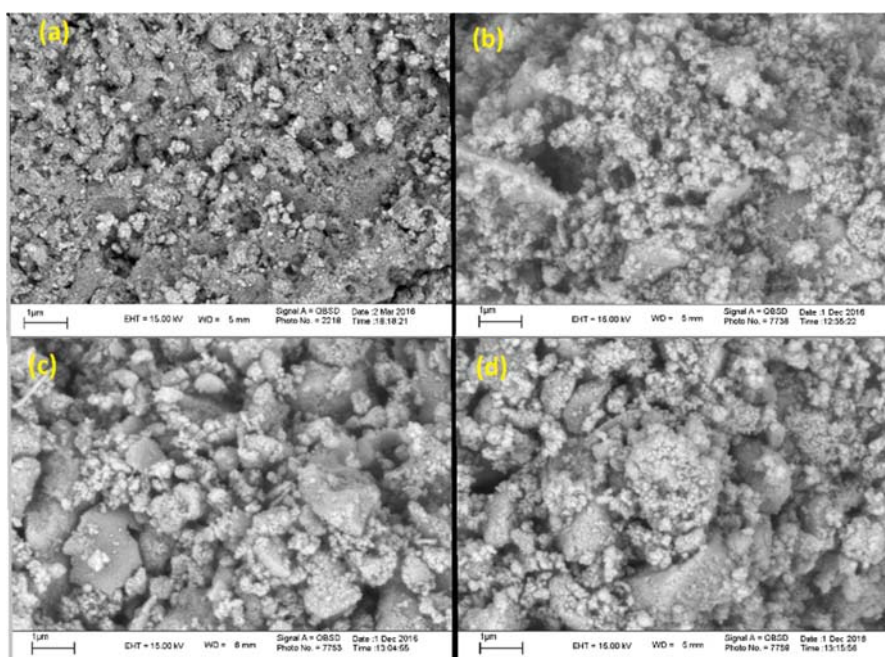

Fig. 4. SEM images of ZCMNPs (a), APTZCMNPs (b), pyr/APTZCMNPs(c) and Co@pyr/APTZCMNPs (d).

3.1.5. TEM analysis

Transmission electron microscopy was used to survey the structure and morphology of the prepared materials. The TEM image in Fig. 5 exhibits that the Co@pyr/APTZCMNPs nanoparticles are of almost spherical shape with a narrow size distribution (the average particle size is 28 nm).

3.1.6. EDX analysis

The elemental composition of the Co@pyr/APTZCMNPs nanocatalyst was performed by the EDX (energy dispersive X-ray) analysis (Fig. 6). The EDX analysis demonstrated the existence of cobalt, iron, carbon and silicon in the structure of Co@pyr/APTZCMNPs catalyst confirming catalyst preparation successfully.

In continuation of our interest in the synthesis of heterocyclic compounds [29-35], we reported our results on the efficient and rapid synthesis of 14*H*-dibenzo[*a.j*]xanthenes using Co@pyr/APTZCMNPs as a novel, efficient and reusable heterogeneous catalyst under solvent-free conditions (Scheme 2). Initially, we investigated the one-pot condensation of benzaldehyde with β-naphthol in the presence of Co@pyr/APTZCMNPs as a model reaction. To exploit optimum conditions for this model reaction, first the effect of solvents, amounts of catalyst and temperatures were surveyed and optimized.

For this purpose, a condensation between benzaldehyde (1 mmol) and β-naphthol (2 mmol) was required (Table 1). To obtain the optimal reaction solvent, several classic solvents such as H_2O, CH_2Cl_2, CH_3CN, DMF, toluene and EtOH in the presence of a certain amounts of catalyst were chosen as the medium for comparison (Table 1, entries 1-6). Among the tested solvents, EtOH produced a high percentage of the product (Table 1, entry 6), but the formation of 14-(phenyl)-14*H*-dibenzo[*a,j*]xanthene was more facile and proceeded in high yield under solvent-free conditions (Table 1, entry 7). To discover for the optimal optimum amount of catalyst, the reactions were performed at different amount of the catalyst ranging from 5-15 mg (Table 1, entries 8-9). With the optimization of catalyst amount, we explored that 10 mg of Co@pyr/APTZCMNPs could effectively catalyze the reaction for preparation of the desired product in short time. It was observed that the yields of the product were not improved as the reaction catalyst was raised (Table 1, entry 9) whereas the lower amount of the catalyst was reduced the reaction efficiency (Table 1, entry 8). In the absence of the catalyst, 14-(phenyl)-14*H*-dibenzo[*a,j*]xanthene was achieved in trace yield after 80 min (Table 1, entry 10). The effect of temperature was surveyed by doing the model reaction in the presence of Co@pyr/APTZCMNPs (10 mg) at various temperatures.
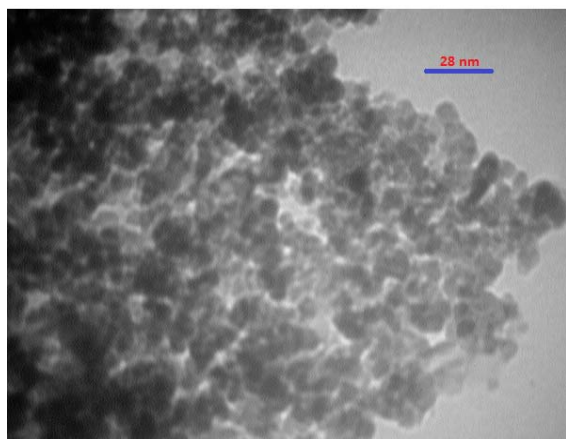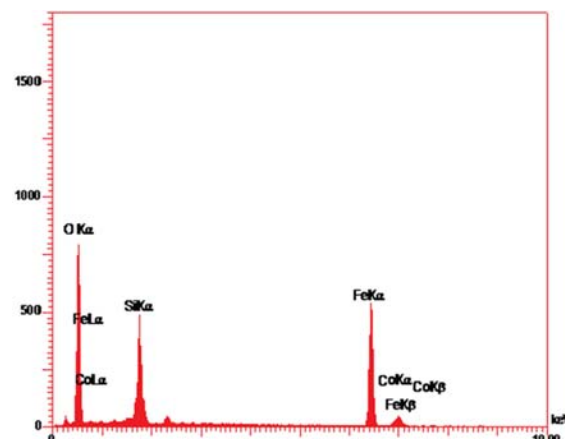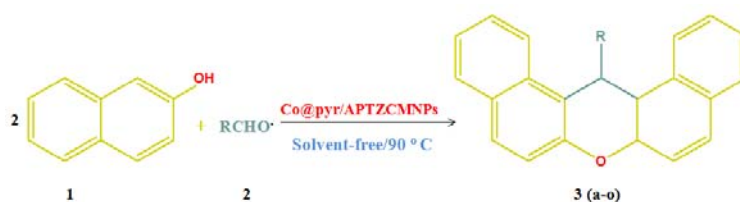

Fig. 5. TEM image of Co@pyr/APTZCMNPs.

Fig. 6. EDX spectrum of Co@pyr/APTZCMNPs.

Scheme 2. The synthesis of xanthene derivatives in the presence of Co@pyr/APTZCMNPs under solvent-free conditions.

Table 1. Effect of the solvent, temperature, reaction time and the amount of the catalyst in the synthesis of 14*H*-dibenzo[*a.j*]xanthenes.

Entry	Solvent	Catalyst (mg)	Temp.	Time (min)	Yield (%)
1	CH_2Cl_2	10	Reflux	80	51
2	CH_3CN	10	Reflux	80	58
3	toluene	10	Reflux	80	57
4	DMF	10	Reflux	80	61
5	H_2O	10	Reflux	80	68
6	EtOH	10	Reflux	80	72
7	Solvent-free	10	90 °C	9	89
8	Solvent-free	5	90 °C	9	75
9	Solvent-free	15	90 °C	9	86
10	Solvent-free	-	90 °C	80	trace
11	Solvent-free	10	25 °C	9	34
12	Solvent-free	10	70 °C	9	76
13	Solvent-free	10	100 °C	9	87

[a]benzaldehyde (1 mmol) and β-naphthol (2 mmol).

To further improve the product yields, we attempted to conduct the experiments in 25, 70, 90 and 100 °C (Table 1, entries 7 and 11-13).

It was observed that a lower reaction temperature led to a lower yield (Table 1, entry 11). After optimizing the reaction, it was observed that 90 °C was the suitable temperature to perform the reaction in short time with high yields (Table 1, entry 7).

Encouraged by this success (Table 1, entry 7), we investigated the generality of this method with various aldehydes to prepare a series of 14*H*-dibenzo [*a.j*] xanthenes (Table 2).

Table 2. Synthesis of 14*H*-dibenzo [*a.j*] xanthene derivatives.[a]

Entry	Aldehyde	Time (min)	Yield (%)[b]	m.p. (°C) Found	m.p. (°C) Reported	Ref.
1	C_6H_5	9	89	184-186	184-185	[36]
2	$2\text{-Cl-}C_6H_4$	5	93	212-214	214-215	[36]
3	$3\text{-Cl-}C_6H_4$	7	90	210-212	209-211	[38]
4	$4\text{-Cl-}C_6H_4$	5	95	289-291	287-288	[36]
5	$3\text{-Br-}C_6H_4$	6	91	193-196	194-195	[39]
6	$4\text{-Br-}C_6H_4$	5	96	298-300	297	[39]
7	$4\text{-F-}C_6H_4$	4	96	237-29	239-240	[36]
8	$2\text{-}NO_2\text{-}C_6H_4$	4	93	212-215	214-215	[36]
9	$3\text{-}NO_2\text{-}C_6H_4$	7	91	205-207	210-211	[36]
10	$4\text{-}NO_2\text{-}C_6H_4$	4	95	319-321	324	[37]
11	$2\text{-MeO-}C_6H_4$	13	90	259-262	260	[40]
12	$3\text{-MeO-}C_6H_4$	15	87	175-177	179-180	[39]
13	$4\text{-MeO-}C_6H_4$	11	88	204-204	203-206	[42]
14	$3\text{-Me-}C_6H_4$	16	87	197-199	198	[39]
15	$4\text{-Me-}C_6H_4$	12	89	225-228	227-228	[36]

[a]All products were characterized by ^{1}H NMR, ^{13}C NMR and IR spectral data and comparison of their melting points with those of authentic samples.
[b]Isolated yield.

Electron-withdrawing and electron-donating as well as halogen substituents on the aldehydes reacted very well to give the corresponding xanthenes with high purity in good-to-excellent yields (Table 2 entries 1-15). More accurate analysis demonstrated that aryl aldehydes with electron-donating group react slower toward aryl aldehydes with electron-withdrawing groups (Table 2 entries 11-15).

To illustrate the merit of using the catalyst (Co@pyr/APTZCMNPs) to synthesize 14*H*-dibenzo[*a.j*] xanthenes in comparison with other catalysts reported for similar reactions, we tabulated several results in Table 3. It is clear that our method is a simpler, more efficient, and the reaction completed within a short period of time than other catalysts used in the references.

A reasonable pathway for the synthesis of xanthane derivatives (4a-o) catalyzed by Co@pyr/APTZCMNPs is proposed (Scheme 3). The reaction of β-naphthol **1** in its enol form is anticipated to react with aromatic aldehyde **2**, under the influence of Co@pyr/APTZCMNPs, to give the intermediate **4** by Knoevenagel adduct formation. The intermediate **4** may further undergo Michael addition with another molecule of β-naphthol, followed by cyclization to give the intermediate **5**. The final product **3** was then formed by cyclization and dehydration of the intermediate **5** (Scheme 3).

Table 3. Comparison of our results with those obtained by other groups to synthesize of 14-(phenyl)-14*H*-dibenzo [*a,j*] xanthene.

Entry	Condition	Catalyst	Time (min)	Yield (%)	Ref.
1	Neat/125 °C	*p*-TSA	240	89	[40]
2	Neat/125 °C	Sulfamic acid	480	93	[43]
3	Neat/125 °C	$K_5CoW_{12}O_{40}$-3H$_2$O	120	91	[24]
4	Neat/90 °C	I_2	150	90	[25]
5	Neat/110-115 °C	Cellulose sulfuric acid	90	81	[28]
6	Neat/90 °C	Co@pyr/APTZCMNPs	9	89	This work
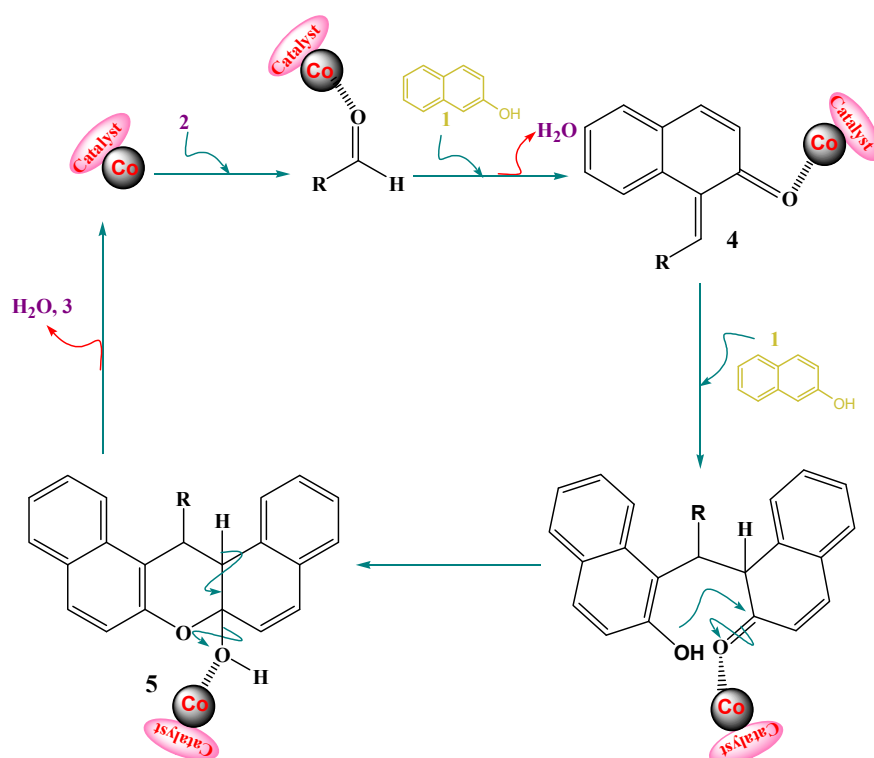
Scheme 3. The plausible mechanism of the reaction.

4. Conclusion

In conclusion, we introduced a straightforward, efficient, and cost-effective synthesis of pyrimido14*H*-dibenzo[*a,j*]xanthenes derivatives in the presence of strong solid acid catalyst Co@pyr/APTZCMNPs under solvent-free conditions. High yields, short reaction time, simplicity of operation, and easy workup are some advantages of the presented approach.

Acknowledgements

References

[1] V. Polshettiwar, R. Luque, A. Fihri, H. Zhu, M. Bouhrara, J. M. Basset, Chem. Rev. 111 (2011) 3036-3075.

[2] N. Kalvari Janaki, R. Fazaeli, H. Alyari, Iran. J. Catal. 5 (2015) 49-56.

[3] R. Cano, D.J. Ramon, M. Yus, Tetrahedron 67 (2011) 5432-5436.

[4] B. Baruwati, V. Polshettiwar, R.S. Varma, Tetrahedron Lett. 50 (2009) 1215-1218.

[5] J. Liu, X. Peng, W. Sun, Y. Zhao, C. Xia, Org. Lett. 10 (2008) 3933-3936.

[6] M. Kooti, M. Afshari, Catal. Lett. 142 (2012) 319-325.

[7] S. Paul, J.H. Clark, J. Mol. Catal. A: Chem. 215 (2004) 107-111.

[8] S. Singh, B.C. Yadav, V.D. Gupta, P.K. Dwivedi, Mater. Res. Bull. 47 (2012) 3538-3547.

[9] S. Sultana, M. Zain Khan, K. Umar, J. Alloys Compd. 535 (2012) 44-49.

[10] J.Y. Ho, S.S. Deok, S.H. Woo, P.K. Soo, K.D. Wan, Nanotechnology 23 (2012) 125402-125407.

[11] C. Barcena, A.K. Sra, G.S. Chaubey, C. Khemtong, J.P. Liu, J. Gao, Chem. Commun. 19 (2008) 2224-2226.

[12] A. Jordan, R. Scholz, P. Wust, H. Fahling, F. Roland, J. Magn. Magn. Mater. 201 (1999) 413-419.

[13] T. Hideo, Jpn. Tokkyo Koho (1981) JP 56005480.

[14] R.W. Lambert, J.A. Martin, J.H. Merrett, K.E.B. Parkes, G.J. Thomas, PCT Int. Appl. (1997) WO 9706178.

[15] J.P. Poupelin, G. Saint-Rut, O. Foussard-Blanpin, G. Narcisse, G. Uchida-Ernouf, R. Lacroix, Eur. J. Med. Chem. 13 (1978) 67-71.

[16] R.M. Ion, D. Frackowiak, A. Planner, K. Wiktorowicz, Acta Biochim. Pol. 45 (1998) 833-845.

[17] A. Banerjee, A.K. Mukherjee, Stain Technol. 56 (1981) 83-85.

[18] M. Ahmad, T.A. King, D.K. Ko, B.H. Cha, J. Lee, J. Phys. D: Appl. Phys. 35 (2002) 1473-1476.

[19] C.G. Knight, T. Stephens, Biochem. J. 258 (1989) 683-689.

[20] R.N. Sen, N. Sarkar, J. Am. Chem. Soc. 47 (1925) 1079-1091.

[21] P. Papini, R. Cimmarusti, Gazz. Chim. Ital. 7 (1947) 142-145.

[22] B. Rajitha, B. Sunil Kumar, Y.T. Reddy, Y.N. Reddy, N. Sreenivasulu, Tetrahedron Lett. 46 (2005) 8691-8693.

[23] K. Ota, T. Kito, Bull. Chem. Soc. Jpn. 49 (1976) 1167-1168.

[24] L. Nagarapu, S. Kantevari, V.C. Mahankhali, S. Apuri. Catal. Commun. 8 (2007) 1173-1177.

[25] B. Das, B. Ravikanth, R. Ramu, K. Laxminarayana, B. Rao-Vittal, J. Mol. Catal. A: Chem. 255 (2006) 74-77.

[26] A. Saini, S. Kumar, J.S. Sandhu, Synlett (2006) 1928-1932.

[27] S. KO, C.F. Yao, Tetrahedron Lett. 47 (2006) 8827-8829.

[28] J.V. Madhav, V.T. Reddy, P.N. Reddy, M.N. Reddy, S. Kumar, P.A. Crooks, B. Rajitha, J. Mol. Catal. A: Chem. 304 (2009) 85-87.

[29] E. Abbaspour-Gilandeh, M. Aghaei-Hashjin, A. Yahyazadeh, H. Salemi, RSC Adv. 6 (2016) 55444-55462.

[30] E. Abbaspour-Gilandeh, S.C. Azimi, A. Mohammadi-Barkchai, RSC Adv. 4 (2014) 54854-54863.

[31] E. Abbaspour-Gilandeh, M. Aghaei-Hashjin, P. Jahanshahi, M. Hoseininezhad, Monatsh Chem. 148 (2017) 731-738.

[32] K. Rad-Moghadam, S.C. Azimi, E. Abbaspour-Gilandeh, Tetrahedron Lett. 54 (2013) 4633-4636.

[33] A. Khorshidi, K. Tabatabaeian, H. Azizi, M. Aghaei-Hashjin, E. Abbaspour-Gilandeh, RSC Adv. 7 (2017) 17732-17740.

[34] E. Abbaspour-Gilandeh, S.C. Azimi, K. Rad-Moghadam, A. Mohammadi-Barkchai, Iran. J. Catal. 3 (2013) 15-20

[35] E. Abbaspour-Gilandeh, S.C. Azimi, K. Rad-Moghadam, A. Mohammadi-Barkchai, Iran. J. Catal. 2 (2013) 91-97.

[36] D. Fang, K. Gong, Z.L. Liu, Catal. Lett. 127 (2009) 291-295.

[37] A. Khoramabadi-Zad, Z. Kazemi, H. Amiri Rudbari, J. Korean Chem. Soc. 46 (2002) 541-544.

[38] S. Kantevari, M. Venu Chary, A.P. Rudra Das, S.V.N. Vuppalapati, N. Lingaiah, Catal. Commun. 9 (2008) 1575-1578.

[39] S. Rostamizadeh, N. Shadjou, A.M. Amani, S. Balalaie, Chin. Chem. Lett. 19 (2008) 1151-1155.

[40] A.R. Khosropour, M.M. Khodaei, H. Moghannian, Synlett (2005) 955-958.

[41] A.K. Bhattacharya, K.C. Rana, M. Mujahid, I. Sehar, A. K. Saxena, Bioorg. Med. Chem. Lett. 19 (2009) 5590-5593.

[42] M. Hong, C. Cai, J. Fluorine Chem. 130 (2009) 989-992.

[43] B. Rajitha, B. Sunil Kumar, Y. Thirupathi Reddy, Y. Narasimha Reddy, N. Sreenivasulu, Tetrahedron Lett. 46 (2005) 8691-8693.